Characterization of a Turbo-Switch SOA Wavelength Converter Using Spectrographic Pulse Measurement

Douglas A. Reid, Aisling M. Clarke, *Student Member, IEEE*, Xuelin Yang, *Member, IEEE*, Robert Maher, *Student Member, IEEE*, Roderick P. Webb, Robert J. Manning, *Member, IEEE*, and Liam P. Barry, *Member, IEEE*

***Abstract*—We use the frequency-resolved optical gating (FROG) technique to determine the pulsewidth and chirp characteristics of wavelength-converted pulses from a turbo-switch and asymmetrical Mach–Zehnder filter combination under a variety of operating conditions. The output pulses were found to be near transform limited and had a high tolerance to line rate and input power variations.**

***Index Terms*—High-speed optical techniques, optical frequency conversion, optical pulse measurement, semiconductor optical amplifiers, wavelength conversion.**

I. Introduction

With the increasing demand for greater transmission bandwidths and the large variety of applications for which this bandwidth is used, it is of great importance to have networks capable of dynamic reconfiguration [1]. This enables the networks to be adapted to the changing requirements placed upon them by users. The recent demand for greater network flexibility in optical networks has led to developments in tuneable laser technology, reconfigurable add drop multiplexers (ROADMs), and optical crossconnects. One important component in future optical networks is an all-optical wavelength converter. These are required to avoid wavelength contention at nodes and to enable wavelength division multiplexing (WDM) systems to be more flexible [2].

There are numerous approaches to wavelength conversion, including four wave mixing (FWM) in fiber [3], semiconductor optical amplifiers (SOAs) [4], [5], and $LiNbO_3$ waveguides [6]; and also cross phase modulation (XPM) and cross gain modulation (XGM) in SOAs [7]–[9].

In this paper, we build on previous work and present an analysis of the turbo-switch wavelength conversion scheme [8], [9] using spectrographic pulse measurement. The operation of the turbo-switch, described in [10], enables very high bit rate operation as it overcomes the nonlinear patterning typically associated with SOA wavelength converters. Characterization of the pulse shape and chirp generated due to the turbo-switch in conjunction with a delayed interferometer (DISC) is described in [11]. Here, we focus on this work and examine in more detail the evolution of the pulse shape and chirp as a function of the turbo-switch configuration. A second harmonic generation (SHG) frequency-resolved optical gating (SHG-FROG) setup was used to analyze the pulses. The FROG technique was first proposed by Trebino and Kane [12], and, since then, it has been used to measure optical pulses in a wide spectral range (from the visible to the near-infrared) and wide range of repetition frequencies [low repetition rate passively mode-locked sources to high repetition rate (170 Gb/s) communications pulses]. The FROG works by making a measurement of a spectrographic representation of the pulse. From this spectrogram, it is then possible to extract the complex amplitude (intensity and phase) of the optical pulse, without any assumption about its shape or structure. There are a wide variety of techniques for the measurement of spectrograms, which are distinguished by the gating process (in our case SHG). In SHG-FROG, a nonlinear crystal is used in an autocorrelator configuration to temporally gate the pulse. The resulting gated pulse is spectrally resolved using a spectrometer. The SHG-FROG setup used here consisted of a noncollinear Michelson interferometer in conjunction with a lithium niobate crystal with a thickness of 1 mm to form the autocorrelator. This was followed by a 300 mm double pass Czerny–Turner spectrometer with a 1200 lines/mm diffraction grating and a 1024 element charge-coupled device (CCD) array. The resulting FROG had a delay resolution of 16 fs (1 μm) and a spectral resolution of 0.025 nm (12.5 GHz) at 775 nm. Spectrographic measurements were taken on a 128×128 grid and were inverted using a principal component generalized projections (PCGPs) algorithm [13]. A low dispersion erbium-doped fiber amplifier (EDFA) suitable for amplifying short pulses was used to achieve the optical powers required to make the FROG measurements. Previous experiments have shown that this amplifier has no significant effect on the intensity and phase profile of the amplified pulse.

In Section II, we outline the turbo-switch configuration used for high-speed wavelength conversion, and highlight its advantages over a single SOA configuration. Examples of pulse outputs from both setups are compared. Section III discusses two implementations of an asymmetric Mach–Zehnder interferometer (AMZI), which uses the XPM from the turbo-switch to invert the wavelength-converted signal [14]. The two approaches are: the use of a polarization maintaining fiber (PMF) and polarizer combination and a planar silica AMZI. The optimal length

Manuscript received November 1, 2007; revised January 22, 2008. This work was supported by the Science Foundation Ireland under Grants 03/IN.1/1340, 06/IN/I969, and 02/IN.1/142.

D. A. Reid, A. M. Clarke, R. Maher, and L. P. Barry are with the Research Institute for Networks and Communications Engineering (RINCE), School of Electronic Engineering, Dublin City University, Dublin 9, Ireland (e-mail: douglas.reid@eeng.dcu.ie; clarkea@eeng.dcu.ie; robert.maher@eeng.dcu.ie; liam.barry@dcu.ie).

X. Yang, R. P. Webb, and R. J. Manning are with the Photonic Systems Group, Tyndall National Institute, Cork, Ireland (e-mail: xuelin.yang@tyndall.ie; rod.webb@tyndall.ie; bob.manning@tyndall.ie).

Color versions of one or more of the figures in this paper are available online at http://ieeexplore.ieee.org.

Digital Object Identifier 10.1109/JSTQE.2008.919742

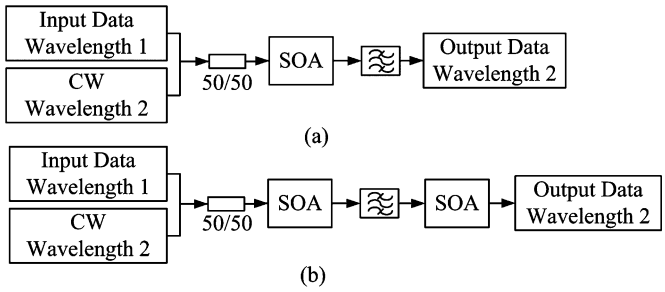

Fig. 1. Experimental setups for SOA-based wavelength conversion. (a) Single SOA approach. (b) Turbo-switch.

and position of the PMF to give the best converted pulse is investigated. Section IV demonstrates the use of the wavelength converter up to 170 Gb/s, and shows how the output pulse shape and phase are insensitive to variations in the line rate and input power. Finally, Section V compares the experimental results with numerical modeling.

II. Comparison Between Single SOA and Turbo-Switch

The simplest approach to wavelength conversion uses a single SOA, as shown in Fig. 1(a). The input data signal at wavelength 1 is combined with a continuous wave (CW) signal at the desired output wavelength. If the data signal has sufficient power, then the data pulses modulate the CW signal through the XGM. In this case, the maximum data rate is limited by the band-filling recovery time of the SOA (typically > 50 ps).

One technique for overcoming this limitation, called the turbo-switch [10], works by filtering out the pump signal after the first SOA and only allowing the modulated CW signal to reach a second SOA. Self-gain modulation in the second SOA causes the gain to recover while the modulated CW is low, and to fall as the modulated CW is recovers. Because of the finite gain recovery time of the second SOA, this self-gain modulation compensates the slow trailing edge in the modulated CW signal while leaving the short initial part largely unchanged. Fig. 1 shows the setups for both single SOA (a) and turbo-switch (b) configurations.

On its own, wavelength conversion based on XGM results in the converted signal being inverted with respect to the input. This is not desirable in return-to-zero (RZ) systems because it leads to a significant increase in the pulse duty cycle. One approach to preserving the polarity of the input signal is to use a shifted bandpass filter at the output of the SOA to suppress the large CW component [15], [16]. There are also several interferometric techniques for inverting the wavelength-converted pulses, the simplest of which is the use of an AMZI [14] (also referred to as a DISC [17]), which relies on the XPM from the SOA. A standard laboratory technique to realize an AMZI is to exploit the birefringence of PMF [18]. The modulated CW probe signal is launched with its polarization at 45° to the fast and slow axes of the fiber. The differing times-of-flight create a switching window where the output is determined by the phase differences between the two orthogonally polarized

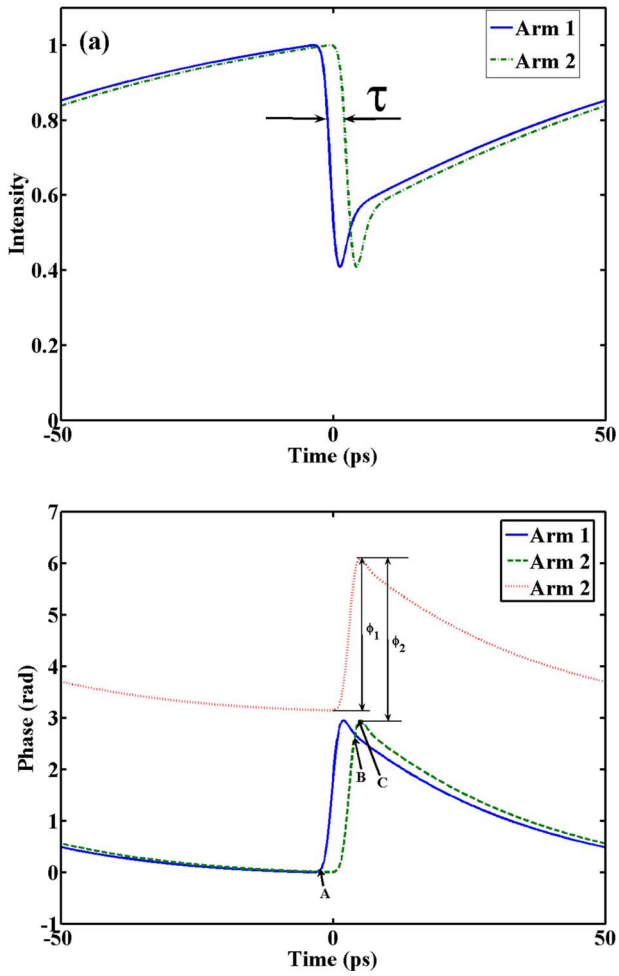

Fig. 2. Modeled intensity (a) and phase (b) of modulated CW signal from SOA for the two arms of the interferometer. The phase of the delayed electric field is shown in two positions, first with the delay equal to an integer multiple of the wavelength (dashed) and second with a subwavelength path difference (dotted) as is optimal.

components, when these interfere at a polarizer. The switching window width may be varied by using different lengths of PMF.

Fig. 2 shows pictorially the intensity (a) and phase (b) of the modulated CW signal after experiencing XGM and XPM in the SOA. A version of this response delayed by the AMZI switching window τ is also shown. Two factors that have a large impact on the quality of the output pulses are the depth of the phase modulation supplied by the SOA(s), denoted here by ϕ_1 and the subwavelength path difference of the interferometer denoted by ϕ_2.

To obtain the greatest extinction, these should both be approximately π. ϕ_1 is a function of the input peak power, while ϕ_2 is controlled by a piezoelectric fiber stretcher in the PMF and a thermal phase shifter in the planar silica AMZI (see Section III-B). Fig. 2(b) also shows that at points A and B, destructive interference will result in minima in the output intensity, while the small phase difference at point C will result in a small satellite pulse.

The shape and chirp of the output pulse is further complicated by the gain recovery and the slight unbalanced power splitting in the interferometer. Fig. 3 shows the implementation of such a

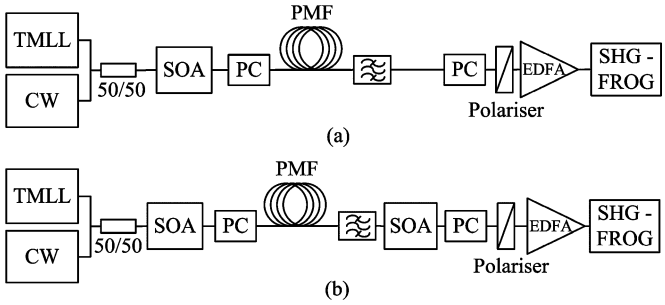

Fig. 3. Use of PM fiber and a polarizer to act as an AMZI to invert the XGM output. (a) From a single SOA. (b) From the turbo-switch.

scheme in the case of a single SOA (a) and the turbo-switch (b). In both the cases, a section of PMF with a 3 ps differential delay was used to implement a DISC. The pump laser source was a tuneable, mode-locked laser (TMLL) running at 1540 nm, delivering 2.5 ps pulses at 10 GHz. This output was used either as a clock pump, or was modulated with PRBS of length $2^7 - 1$. It was possible to passively multiplex this output up to 170 Gb/s. The FROG measurements of the PRBS pulses were possible with the assumption that every pulse in the pattern was identical. While patterning would negate this assumption, the earlier demonstration of 170 Gb/s error free performance of the turbo-switch [10], and eye measurements, indicated that there was very little patterning in the turbo-switch output. The results given here are for the PRBS case; however, using a simple clock pump (all 1's) was found to give similar results. The average power of the data pulses was 5 dBm at 170 Gb/s and was reduced by 3 dB for each decrease in line rate. The CW beam was at 1558 nm, with a power of 0 dBm. The SOAs were bulk devices, running at 400 mA bias current.

A polarization controller (PC) was used before the PMF to ensure that equal optical power was coupled to the fast and slow axes. A second PC was placed before the output polarizer.

Fig. 4 shows examples of the output pulses from the two configurations that were measured using an SHG-FROG apparatus [12]. Fig. 4(a) shows that the turbo-switch results in a slightly slower rising edge, but a significant sharpening in the trailing edge compared to the case of the single SOA.

The DISC exploits the phase shift generated by the SOA, and since both polarizations experience a similar (but delayed) phase shift, the superposition of these two electric fields results in a phase that increases almost linearly across the output pulse. This results in a pulse with very little chirp, as is shown in Fig. 4(b). There is a small improvement in the magnitude of the chirp across the pulse associated with the turbo-switch configuration in comparison to the SOA and DISC alone.

The improvements in the pulse shape and chirp profile improvement are due to the ultrafast gain recovery time associated with the turbo-switch [16]. Note the significant chirp in the wings of the pulse. This is expected theoretically, and arises from the reversal of the phase differences between the two interfering components at the AMZI output. There is actually no power in the pulse at these points, so the presence of the chirp is of little consequence.

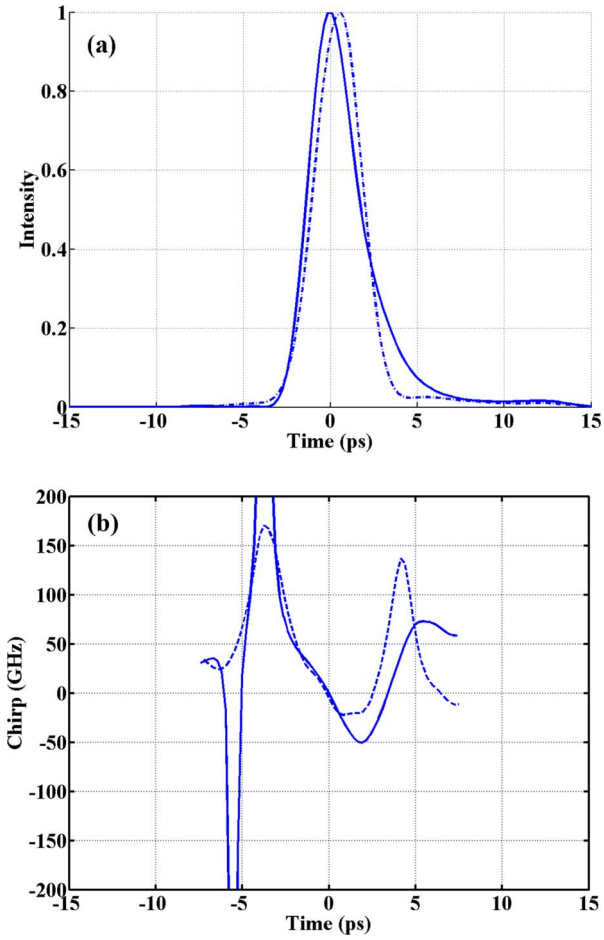

Fig. 4. Comparison of pulses from single SOA with DISC (solid) and turbo-switch (dashed) configurations of wavelength converter. (a) Intensity. (b) Chirp.

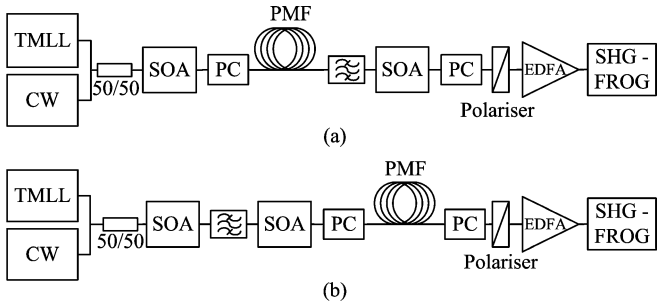

Fig. 5. Two possible placement positions for the PMF in the turbo-switch. (a) Between SOAs. (b) After both SOAs.

III. Implementations of an AMZI

A. Comparison of Placement Position of PMF

Normally, with a single SOA, the PMF and polarizer must be placed after the SOA. However, with the turbo-switch, there are two options for the placement of the fiber, either after the first SOA in the arrangement or after both SOAs (see Fig. 5).

The effect of changing both the position and length of the PMF was investigated experimentally. Fig. 6 shows the results from such a comparison. We observe that there is a slight advantage in

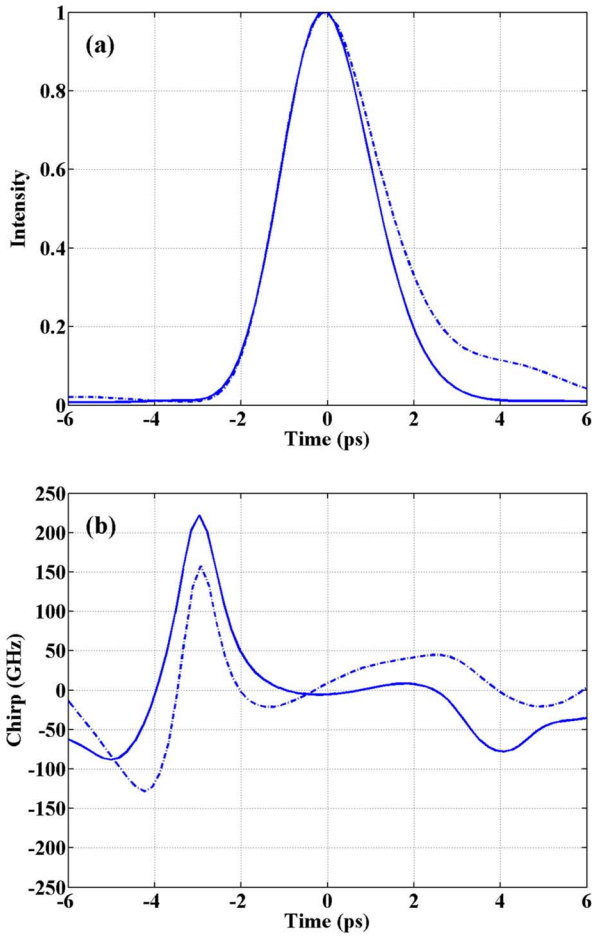

Fig. 6. Comparison of pulses from turbo-switch wavelength converter with PMF between the SOAs (solid) and PMF after the second SOA (dashed). (a) Intensity. (b) Chirp.

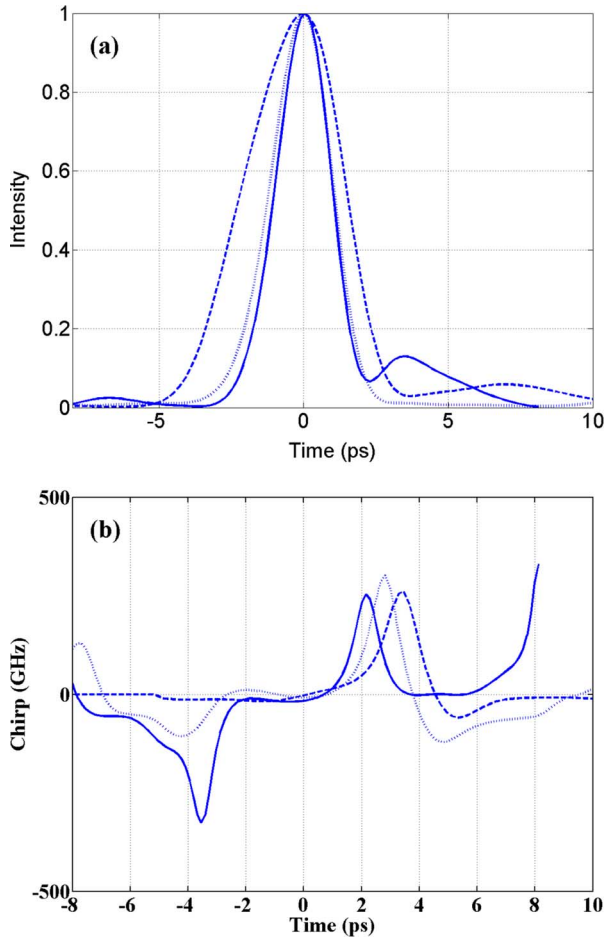

Fig. 7. Comparison of pulses from turbo-switch wavelength converter with 1.9 ps (solid), 3 ps (dotted), and 5 ps (dashed) differential delays in PMF between the SOAs. (a) Intensity. (b) Chirp.

placing the PMF in between the two SOAs, both in pulsewidth and chirp.

However, the pulse quality from configuration of Fig. 5(b) is still very high, showing very little chirp across the center of the pulse. The pulsewidths for the PMF before and after the second SOA were 2.46 and 2.72 ps, respectively.

This improvement is due to the fact that when the PMF is between the two SOAs, the delayed polarization experiences slightly more gain and a slightly reduced phase shift. This results in a reduction of the phase overshoot shown at point C in Fig. 2, and a corresponding reduction in trailing artifacts in the output pulse.

We also show in Fig. 7 the effect of varying the switching window width, for configuration in Fig. 5(a). Clearly the output pulsewidth varies with switching window width, but it is also dependent on the gain recovery time of the SOA. The turbo-switch has a gain recovery time of 3 ps (dependent on operating conditions), and thus, we believe that the optimum performance was achieved with the 3 ps switching window. Although improved performance can be achieved by optimizing various parameters, the results show generally that there are no consequential large changes to the chirp profile and that it always has a very low value for the range of window widths used.

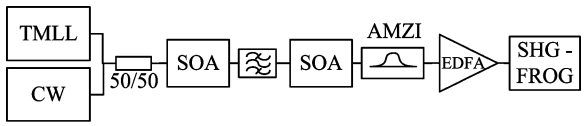

Fig. 8. Use of an AMZI after the turbo-switch.

The effect of reducing the differential delay from 3 to 1.9 ps results in the pulsewidth changing from 3.95 to 2.18 ps for a pump pulsewidth of 2.5 ps. A differential delay of 1.9 ps is suitable for wavelength conversion of 170 Gb/s data, where the pulsewidth should be $<$2.5 ps. The time-bandwidth product is 0.59, indicating that the pulses are nearly transform limited.

B. Planar Silica AMZI

A planar silica AMZI, having a differential delay of 2 ps, was used in the arrangement shown in Fig. 8, and was directly compared with the results using PMF (between SOAs), as shown in Fig. 9.

We again see little difference between the outputs, both schemes achieving high quality pulses. Note that variations in the chirp in the wings are measurement artifacts, and arise due

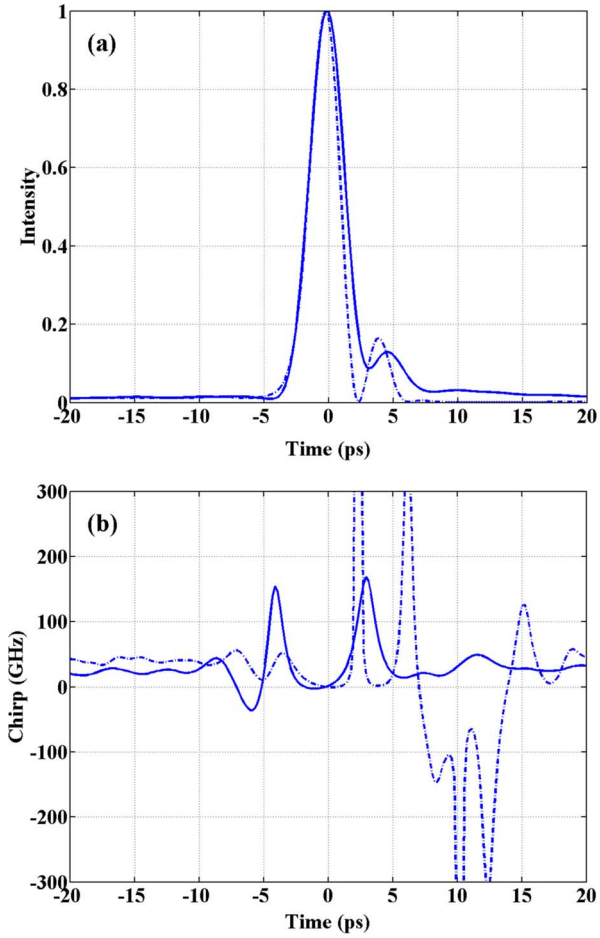

Fig. 9. Comparison of PMF (solid) and AMZI (dashed). (a) Intensity. (b) Chirp.

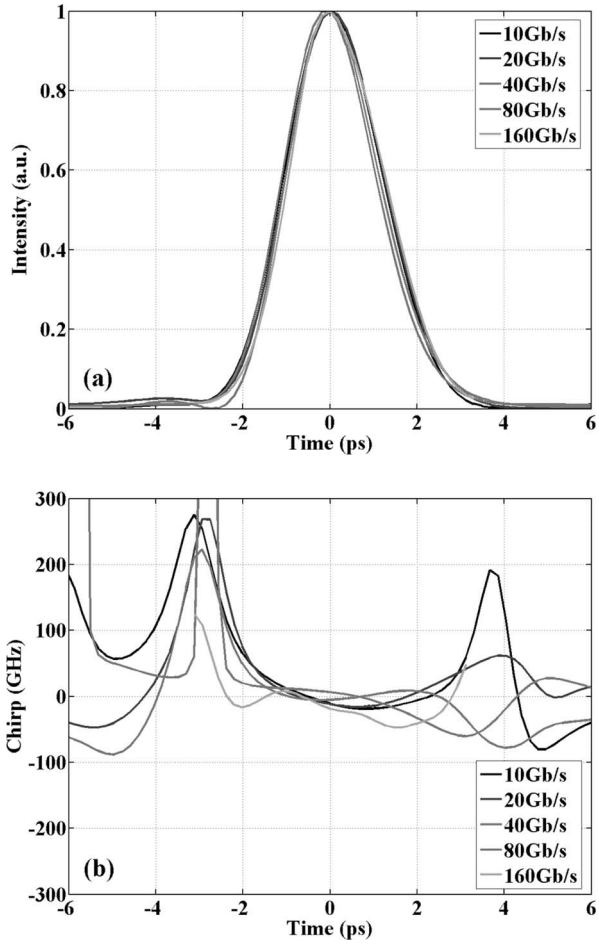

Fig. 10. Comparison of wavelength converted pulses at 10, 20, 40, 80, and 170 Gb/s. (a) Intensity. (b) Chirp.

to the difficulty in extracting meaningful information from the data when the pulse intensity is extremely low. The differences in the appearance of the small trailing pulse are due to slight differences in the phase bias of the interferometers when the measurements were taken.

IV. Wavelength Converter Tolerance

For a wavelength converter to be useful as a practical network element, it will have to work over a range of line rates and variations in the input optical power. The turbo-switch has been shown to operate error free at line rates up to 170.2 Gb/s [10]. For further analysis, the pulses from the wavelength converter were measured using the FROG apparatus for different data rates. For this experiment, the PMF was placed between the two SOAs for a differential delay of 3 ps. The variation in pulsewidth and chirp at line rates from 10 to 170 Gb/s is shown in Fig. 10. It is immediately apparent that there is little variation over this very large range of data rates of either pulsewidth or chirp.

As a further test, the average input power of the pump into the turbo-switch was varied from -7 to 2 dBm. In this case, the data rate was fixed at 40 Gb/s and the PMF (3 ps of differential delay) was placed after the second SOA. The measured pulses are shown in Fig. 11. Once again, the wavelength-converted pulses show very little variation in width, and only a slight increase in chirp despite the input power being varied by almost a factor of 10. These results show the wavelength converter to be very tolerant to system variation.

V. Theoretical Modeling

A turbo-switch with a PMF giving a 3 ps differential delay placed between the SOAs [see Fig. 3(b)] was modeled by numerical simulation. The SOAs were divided into 50 length elements, and the carrier density and temperature in each element were found as a function of time by solving the following rate equations:

$$\frac{dn}{dt} = \frac{I}{eV} - \frac{(n-n_0)k_{\mathrm{CH}}P}{E_{\mathrm{sat}}} - an - bn^2 - cn^3 \quad (1)$$

$$\frac{dk_{\mathrm{CH}}}{dt} = \frac{1 - k_{\mathrm{CH}}(1+\varepsilon S)}{\tau_{\mathrm{CH}}} \quad (2)$$

$$\frac{dP}{dz} = P(\Gamma a_m (n-n_0)k_{\mathrm{CH}} - \alpha) \quad (3)$$

where n is the carrier density, P is the total optical power, and k_{CH} is the carrier heating gain compression factor that is related

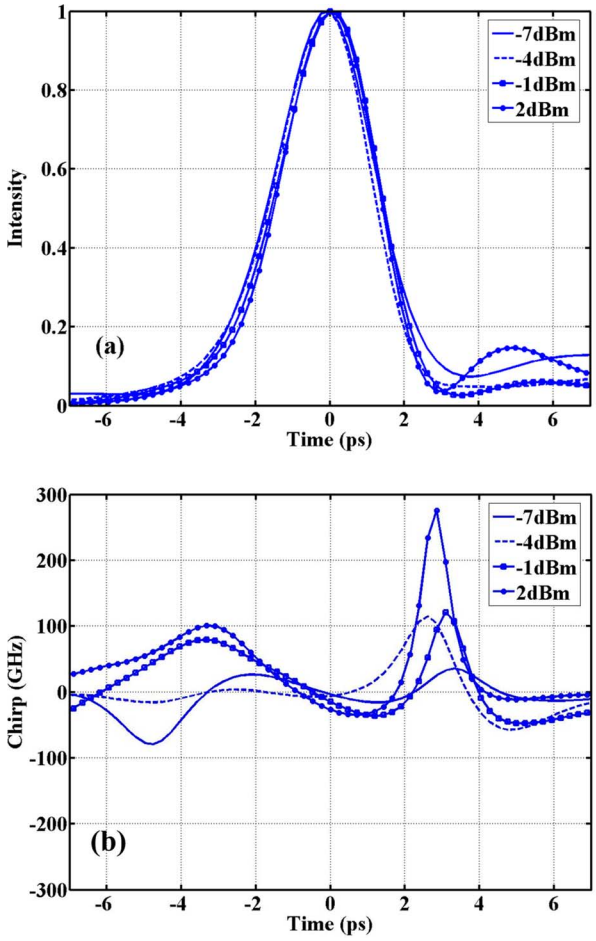

Fig. 11. Effect of changing input pump power on resulting wavelength converted pulse. (a) Intensity. (b) Chirp.

TABLE I
SOA PARAMETERS

Symbol	Quantity	Value
I	Bias current	200mA
V	Active volume	$1.1\text{x}10^{-10}$ cm^3
n_0	Transparency density	10^{18} cm^{-3}
E_{sat}	Saturation energy	1.79pJ
a	Non-radiative recombination coefficient	$4.5\text{x}10^{9}$ s^{-1}
b	Spontaneous recombination coefficient	$1.5\text{x}10^{-10}$ cm^3 s^{-1}
c	Auger recombination coefficient	$1.5\text{x}10^{-28}$ cm^6 s^{-1}
ε	Ultrafast gain compression parameter	$1.5\text{x}10^{-17}$ cm^3
τ_{CH}	Carrier cooling time constant	1ps
Γ	Optical confinement factor	0.175
a_m	Material gain coefficient	$4.5\text{x}10^{-16}$ cm^3
α	Waveguide loss	30 cm^{-1}

to the carrier temperature. n, P, and k_{CH} are functions of both longitudinal position, z, and time, t. S is the photon density obtained from P. e is the electron charge and the remaining symbols are constants defined in Table I.

From the carrier-density and the carrier-heating dependent components of the gain compression, the corresponding phase modulation components were calculated using an alpha factor of 8 for the carrier-density component and 1 for the carrier-heating component [19]. From the gain and phase responses of the two SOAs, the amplitudes and phases of the orthogonally

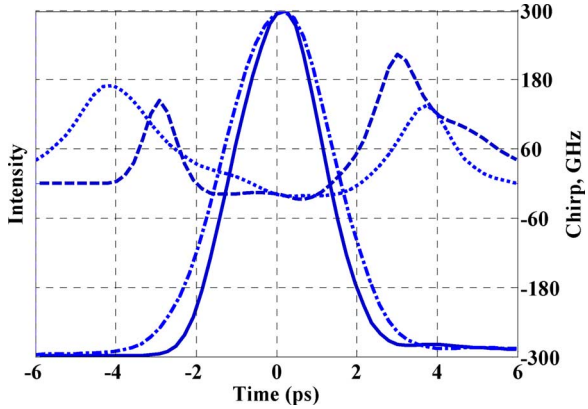

Fig. 12. Modeled (solid line) and measured (dash-dot) output intensity with modeled (dashed line) and measured (dotted) chirp for a turbo-switch with 3 ps differential delay PMF between the SOAs.

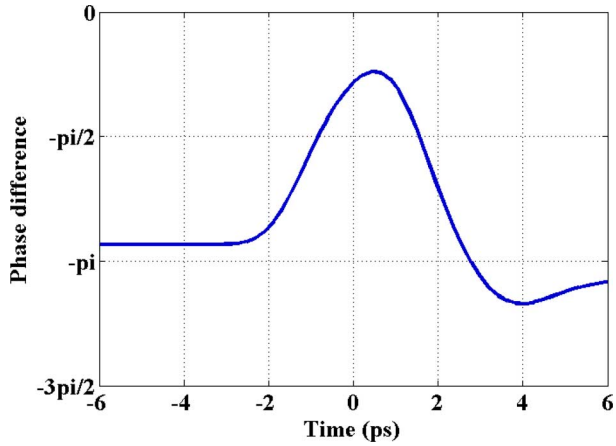

Fig. 13. Modeled phase difference between the orthogonally polarized field components reaching the output polarizer.

polarized fields at the output of the second SOA were obtained, and hence, the resultant field at the output of the polarizer (see Fig. 12). Amplified spontaneous emission was omitted from the model for simplicity. For this reason, it was found that the theoretical results matched the experimental data best when the modeled bias current was set to 200 mA, although 400 mA was used for the experiments.

With this proviso, the modeled pulse intensity was in reasonable agreement with the experimental results, and the chirp showed the same features as the experiment. Just as was observed experimentally, small adjustments to the phase offset of the interferometer could cause substantial changes in the chirp at the wings of the pulse, sometimes accompanied by the appearance of a small trailing intensity pulse. However, large values of chirp only arise when the output intensity of the turbo-switch is small, which occurs when the two field components arriving at the polarizer are approximately equal and are summed in antiphase. In this situation, the output phase is highly sensitive to variations in either component field and can undergo an abrupt reversal. Fig. 13 shows the modeled phase difference between the component fields corresponding to the results in Fig. 12, confirming that the difference is close to π when the chirp is

high. In all cases, low values of chirp in agreement with the measurements were found during the pulse itself.

VI. Conclusion

We have measured the pulsewidth and chirp of wavelength converted pulses from a turbo-switch combined with an AMZI using an SHG-FROG spectrographic technique. The effects of varying the placement and length of PMF to emulate an AMZI within a turbo-switch configuration were studied. These results were also compared with those obtained using a planar silica AMZI. The AMZI that utilized PMF gave a slightly superior performance. We have also compared the effect of varying the repetition rate and power of the data (pump) pulses. In all cases, we observe little sensitivity in the results to such variations, and obtain pulses with very low chirp ($<$20 GHz), which are approximately transform-limited. The results were also found to be in good agreement with a numerical model, and the performance of the turbo-switched-based wavelength converter confirms its suitability for use in future optical networks.

References

[1] C.-C. Sue, "Wavelength routing with spare reconfiguration for all-optical WDM networks," *J. Lightw. Technol.*, vol. 23, no. 6, pp. 1991–2000, Jun. 2005.

[2] S. J. B. Yoo, "Wavelength conversion technologies for WDM network applications," *J. Lightw. Technol.*, vol. 14, no. 6, pp. 955–966, Jun. 1996.

[3] K. Inoue and H. Toba, "Wavelength conversion experiment using fiber four-wave mixing," *IEEE Photon. Technol. Lett.*, vol. 4, no. 1, pp. 69–72, Jan. 1992.

[4] M. C. Tatham, G. Sherlock, and L. D. Westbrook, "20-nm optical wavelength conversion using nondegenerate four-wave mixing," *IEEE Photon. Technol. Lett.*, vol. 5, no. 11, pp. 1303–1306, Nov. 1993.

[5] A. E. Kelly, A. D. Ellis, D. Nesset, R. Kashyap, and D. G. Moodie, "100 Gbit/s wavelength conversion using FWM in an MQW semiconductor optical amplifier," *Electron. Lett.*, vol. 34, no. 20, pp. 1955–1956, Oct. 1998.

[6] M. H. Chou, I. Brener, M. M. Fejer, E. E. Chaban, and S. B. Christman, "1.5-μm-band wavelength conversion based on cascaded second-order nonlinearity in LiNbO3 waveguides," *IEEE Photon. Technol. Lett.*, vol. 11, no. 6, pp. 653–655, Jun. 1999.

[7] T. Durhuus, B. Mikkelsen, C. Joergensen, S. L. Danielsen, and K. E. Stubkjaer, "All-optical wavelength conversion by semiconductor optical amplifiers," *J. Lightw. Technol.*, vol. 14, no. 6, pp. 942–954, Jun. 1996.

[8] Y. Liu, E. Tangdiongga, Z. Li, H. de Waardt, A. M. J. Koonen, G. D. Khoe, X. Shu, I. Bennion, and H. J. S. Dorren, "Error-free 320-Gb/s all-optical wavelength conversion using a single semiconductor optical amplifier," *J. Lightw. Technol.*, vol. 25, no. 1, pp. 103–108, Jan. 2007.

[9] J. Wang, A. Maitra, C. G. Poulton, W. Freude, and J. Leuthold, "Temporal dynamics of the alpha factor in semiconductor optical amplifiers," *J. Lightw. Technol.*, vol. 25, no. 3, pp. 891–900, Mar. 2007.

[10] R. J. Manning, X. Yang, R. P. Webb, R. Giller, F. C. G. Gunning, and A. D. Ellis, "The turbo-switch—A novel technique to increase the high-speed response of SOAs for wavelength conversion," presented at the Opt. Fiber Commun. Conf., Nat. Fiber Opt. Eng. Conf., Mar. 2006, Anaheim, CA, pp. 3.

[11] X. Yang, A. M. Clarke, R. Maher, R. P. Webb, R. J. Manning, and L. P. Barry, "FROG characterisation of a turbo-switch wavelength converter," presented at the Eur. Conf. Opt. Commun., Berlin, Germany, paper PO37, 2007.

[12] D. J. Kane and R. Trebino, "Characterization of arbitrary femtosecond pulses using frequency-resolved optical gating," *IEEE J. Quantum Electron.*, vol. 29, no. 2, pp. 571–579, Feb. 1993.

[13] D. J. Kane, "Real-time measurement of ultrashort laser pulses using principal component generalized projections," *IEEE J. Sel. Topics Quantum Electron.*, vol. 4, no. 2, pp. 278–284, Mar./Apr. 1998.

[14] M. L. Nielsen and J. Mørk, "Increasing the modulation bandwidth of semiconductor-optical-amplifier-based switches by using optical filtering," *J. Opt. Soc. Am. B*, vol. 21, pp. 1606–1619, 2004.

[15] M. L. Nielsen, B. Lavigne, and B. Dagens, "Polarity-preserving SOA-based wavelength conversion at 40 Gbit/s using bandpass filtering," *Electron. Lett.*, vol. 39, no. 18, pp. 1334–1335, Sep. 2003.

[16] A. M. Clarke, G. Girault, P. Anandarajah, C. Guignard, L. Bramerie, L. P. Barry, J. C. Simon, and J. Harvey, "FROG characterisation of SOA-based wavelength conversion using XPM in conjunction with shifted filtering up to line rates of 80 GHz," in *Proc. 19th Annu. Meet. IEEE Lasers Electro-Opt. Soc.*, Oct. 2006, pp. 152–153.

[17] Y. Ueno, S. Nakamura, and K. Tajima, "Nonlinear phase shifts induced by semiconductor optical amplifiers with control pulses at repetition frequencies of the 40–160 GHz range for use in ultrahigh-speed all-optical signal processing," *J. Opt. Soc. Am. B*, vol. 19, no. 11, pp. 1061–1063, May 2006.

[18] N. S. Patel, K. A. Rauschenbach, and K. L. Hall, "40-Gb/s demultiplexing using an ultrafast nonlinear interferometer (UNI)," *IEEE Photon. Technol. Lett.*, vol. 8, no. 12, pp. 1695–1697, Dec. 1996.

[19] R. Giller, R. J. Manning, and D. Cotter, "Gain and phase recovery of optically excited semiconductor optical amplifiers," *IEEE Photon. Technol. Lett.*, vol. 18, no. 9, pp. 1061–1063, May 2006.

Douglas A. Reid received the B.Tech. degree in optoelectronics in 2000 and the Ph.D. degree in physics in 2007 both from the University of Auckland, Auckland, New Zealand.

He is currently with the Radio and Optical Communications Group, Dublin City University, Dublin, Ireland. His current research interests include ultrashort optical pulses, frequency-resolved optical gating (FROG), linear spectrographic techniques for real-time measurement of optical communication pulses, optical pulse generation, and applications of semiconductor optical amplifiers.

Aisling M. Clarke (S'00–M'03) received the B.Eng. and Ph.D. degrees in electronic engineering from Dublin City University, Dublin, Ireland, in 2002 and 2007, respectively.

She is currently with the Research Institute for Networks and Communications Engineering (RINCE), School of Electronic Engineering, Dublin City University. Her current research interests include high-speed all-optical processing techniques with particular emphasis in gigabits per second (Gb/s) wavelength conversion and picosecond pulse generation.

Xuelin Yang (M'05) received the Bachelors' degree in semiconductor physics from Jiangxi University, Jiangxi, China, in 1988, and the Masters' and Ph.D. degrees in optics from the Department of Physics, Shanghai Jiao Tong University, Shanghai, China, in 1992 and 1995, respectively.

He was an Associate Professor at Shanghai Jiao Tong University. During 1999–2001, he was a Postdoctoral Researcher at the Laboratoire Stereo-Chemie de Molecules and Interactions (STIM), Ecole Normale Superieure de Lyon, Lyon, France, where he was engaged in research on organic nonlinear optical materials and devices. From October 2001 to November 2004, he was with the Department of Electrical Engineering, Eindhoven University of Technology, Eindhoven, The Netherlands, where he was engaged in research on ultrafast all-optical switching devices employing semiconductor optical amplifiers in optical telecommunication system. Since 2004, he has been with the Photonics System Group, University College Cork, Cork, Ireland, as Senior Postdoctoral Researcher. His current research interests include all-optical signal processing in telecommunication system.

Robert Maher (S'06) received the B.Eng. degree in electronic engineering from Dublin City University, Dublin, Ireland, in 2005. He is currently working toward the Ph.D. degree with the Radio and Optical Communications Group, Research Institute for Networks and Communications Engineering (RINCE), Dublin City University.

His current research interests include wavelength-tunable pulse generation for hybrid wavelength-division multiplexing optical time division multiplexing (WDM/OTDM) transmission systems.

Roderick P. Webb received the B.Sc. degree in electrical engineering from Imperial College, London, U.K., in 1973, the B.A. degree from the Open University, Milton Keynes, U.K., in 1986, and the Ph.D. degrees in electrical engineering from the Imperial College, in 1993.

He is currently with the Photonic Systems Group, Tyndall National Institute, Cork, Ireland, where he is engaged in research on semiconductor optical amplifiers.

Robert J. Manning (A'01–M'03) received the B.Sc. and Ph.D. degrees in physics from the Imperial College, London, U.K., in 1975 and 1982, respectively.

Earlier he was with Royal Signals and Radar Establishment (RSRE), Malvern, British Telecom Laboratories, Martlesham, and Corning Research Centre, Martlesham. He is currently a Principal Investigator with the Photonic Systems Group, Tyndall National Institute, Cork, Ireland, where he is engaged in research on semiconductor optical amplifiers for all-optical high-speed switching applications. He is the author or coauthor of more than 130 journal and conference papers.

Liam P. Barry (M'98) received the B.E. degree in electronic engineering and the M.Eng.Sc. degree in optical communications from the University College Dublin, Dublin, Ireland, in 1991 and 1993, respectively, and the Ph.D. degree from the University of Rennes, Rennes, France, in 1996.

From February 1993 to January 1996, he was with the Optical Systems Department, France Telecom's Research Laboratories (CNET), Lannion, France, as a Research Engineer. In February 1996, he was with the Applied Optics Centre, University of Auckland, Auckland, New Zealand, as a Research Fellow, where he worked on optical pulse generation and characterization. Since 1998, he has been with the School of Electronic Engineering, Dublin City University, where he has since developed the Radio and Optical Communications Laboratory.